AKADÉMIAI KIADÓ

UNIVERSITY of DEBRECEN

International Review of Applied Sciences and Engineering

14 (2023) 1, 1–12

DOI:
10.1556/1848.2021.00375

ORIGINAL RESEARCH PAPER

Optimum of fractional order fuzzy logic controller with several evolutionary optimization algorithms for inverted pendulum

Ahmed Faisal Ghaleb[1], Ahmed Alaa Oglah[1], Amjad J. Humaidi[1]*, Abdulkareem Sh. Mahdi Al-Obaidi[2] and Ibraheem Kasim Ibraheem[3]

[1] Control and Systems Engineering Department, University of Technology, Iraq

[2] School of Engineering, Faculty of Innovation and Technology, Taylor's University, Malaysia

[3] Computer Engineering Techniques Department, Al-Mustaqbal University College, 51001 Hilla, Iraq

Received: September 7, 2021 • Accepted: December 27, 2021
Published online: September 7, 2022

ABSTRACT

This paper compared the performance between Integer Order Fuzzy PID (IOFPID) and Fractional Order Fuzzy PID (FOFPID) controllers for inverted pendulum system as a controlling plant. The parameters of each controller were tuned with four evolutionary optimization algorithms (Social Spider Optimization (SSO), Swarm Optimization (PSO), Genetic Algorithm (GA), and Particle Ant Colony Optimization (ACO)). The comparisons were carried out between the two controllers IOFPID and FOFPID, as well as among the four optimization algorithms for the two controllers. The results of comparisons proved that the FOFPID controller with SSO has achieved the best time response characteristics and the least tuning time.

KEYWORDS

fuzzy PID, fractional order PID, GA, ACO, PSO, SSO

1. INTRODUCTION

The inverted pendulum system on cart is an outstanding test benchmark for many difficult control seeking issues, as well as a suitable instrument for verifying the capacity of controllers in the control researching field. The inverted pendulum system is a single I/P multi O/P s' (SIMO) method with a single I/P (force exerted on the cart) and two O/Ps' (The angle of inverted pendulum and the car position).

The inverted pendulum system is widely employed in a variety of applications, including rocket launch and missile guidance. The two-wheel scooter (Segway) is a commercial use of the inverted pendulum model. Humanoid robots that walk upright are another implementation of the inverted pendulum concept [1]. In attempt to linearize the system, some academics neglect friction on the mathematical model for an inverted pendulum system [2–4], however, this is not a legal approximation since the cart and the pole of pendulum physically come into touch with each other. Using Lagrange equations to explain the equations of motion, the researchers of [5, 6] gave explicit stages in mathematical modeling to the system. Inverted pendulum control methods and design strategies include the Integer Order Proportional Integral Derivative (IOPID) controller [7], Fuzzy logic controller (FLC) [8–10], and Fractional Order PID (FOPID) controller [11]. The fuzzy controllers were

*Corresponding author.
E-mail: amjad.j.humaidi@uotechnology.edu.iq

integrated with FOPID in [12–14] to produce fuzzy like FOPID controllers. The fine tuning of controller settings is essential, as the controller type might have an impact on the system's stability. As a result, selecting the best settings is also the goal. Parameter tuning can be done in a variety of ways. The first way, as described in [15], is trial and error. This method takes a significant amount of effort and time. Podlubny released a research article [16] that connects control theory with fractional calculus. Many evolutionary optimization techniques, such as Social Spider Optimization (SSO), Particle Swarm Optimization (PSO); Ant Colony Optimization (ACO.); and Genetic Algorithm (GA); are commonly employed (GA). Despite its advantages over other artificial intelligence algorithms, as demonstrated by the results of this research, the SSO is rarely employed to determine parameters with inverted pendulum controllers. This research compares Type-1 Fuzzy Logic Controllers (T1FLC) such as IOPID and Fractional Order Type-1 Fuzzy Logic Controllers (FOT1FLC) such as FOPID, as well as modifying their settings using four evolutionary optimization strategies (GA, PSO, ACO, SSO).

The contributions of this research paper are:

- The fuzzy logic controller has been mixed with fractional order PID controller for governing and controlling the inverted pendulum system on cart.
- Determine the best evolutionary optimization algorithm from the four algorithms (GA, PSO, ACO, and SSO) that were used for tuning and optimising the parameters of FOT1FLC.

This study topic may be easily modified and utilized in a variety of technical fields. The following is how the rest of the article is arranged after the introduction:

Sections 2 presents the mathematical model of inverted pendulum system, section 3 conducts mathematical basis of fractional order calculus, section 4 presents a brief explanation of a fuzzy logic controller, section 5 discusses the suggested optimization techniques, section 6 presents the design of FOFPID controller, section 7 demonstrates the experimental and numerical results, and section 8 highlights the main concluded points based on results.

2. MATHEMATICAL MODEL

The Inverted Pendulum system's mathematical model will be re-derived here using the second kind of Lagrange motion equations. For complex systems, Lagrange equations are the most widely used mechanical and analytical approach for determining the system equation of motion. Figure 1 and Table 1, [17–19], demonstrate the Inverted Pendulum on a cart (Table 2).

The parameters of mathematical model for inverted pendulum system on cart are presented in Table 1 and shown in Fig. 3. The values of the parameters represented the physical values of digital pendulum control instrument experiments system 33-936S, *which were used in real time implementation of research.*

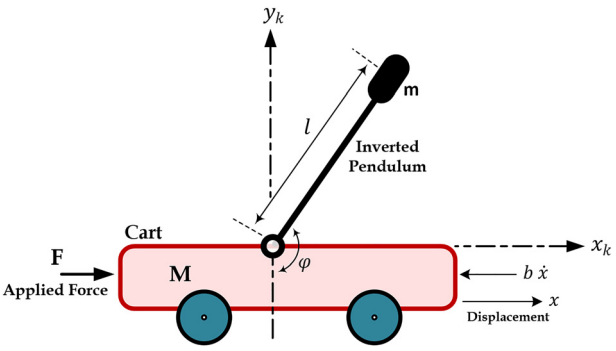

Fig. 1. The cart of inverted pendulum

Table 1. Pendulum system physical parameters

Parameter	Symbol	Value	Unit
Cart mass	M	2.4	Kg
Length of pendulum	l	0.36	m
Penduium mass	m	0.23	Kg
Friction coefficient of pendulum	$b2$	0.005	$Nrad^{-1}s^{-1}$
Friction coefficient of cart	$b1$	0.05	$Nm^{-1}s^{-1}$
Gravitation force	g	9.81	m/s^2
Moment of inertia (Pendulum mass)	I	0.099	$Kg\ /m^2$
Force applied on the cart	F	-	N
Cart Position	X	-	m
Angle of inverted Pendulum system	θ	-	rad

Table 2. PID options are special case of FOPID

λ	μ	Controller
0	0	P
0	1	PI
1	0	PD
1	1	PID

In this study, Lagrangian method is used to develop the dynamic model of the system [20–22]. The kinetic energy law is

$$(\mathrm{KE}) = \frac{1}{2}MV^2 \tag{1}$$

X = Position of cart.

Position derivation X by time is. $\dot{X}\dot{X}$ = cart velocity.

An inverted pendulum's kinetic energy is proportional to the passage of time.

$$E_{KV} = \frac{1}{2}M\dot{X}^2 \tag{2}$$

X_K = The pendulum's horizontal position coordinate.

Y_K = The pendulum's vertical position coordinates.

$$X_K = X + l\sin\theta \tag{3}$$

$$Y_K = l\cos\theta\sin\theta \tag{4}$$

Derivation of positions $(X_K,\ Y_K)$ by time is velocities $(V_{KX},\ Y_{Ky})$

$$V_{KX} = \dot{X} + l\cos\theta \tag{5}$$

$$V_{KY} = -l\dot{\theta}\sin\theta \tag{6}$$

The velocity square for pendulum well be

$$\begin{aligned}\left|V_K^2\right| &= V_{KX}^2 + V_{KY}^2\sin\theta \\ &= \dot{X}^2 + 2l\dot{X}\dot{\theta}i\cos(\theta) + l^2\dot{\theta}^2(\cos(\theta))^2 + l^2\dot{\theta}^2(\sin(\theta))^2 \\ &= \dot{X}^2 + 2l\dot{X}\dot{\theta}i\cos(\theta) + l^2\dot{\theta}^2\end{aligned} \tag{7}$$

Since the kinetic energy of pendulum is

$$E_{KK} = \frac{1}{2}mV^2$$

$$E_{KK} = \frac{1}{2}m\dot{X}^2$$

$$= \frac{1}{2}m\left(\dot{X}^2 + 2l\dot{X}\dot{\theta}\cos\theta + l^2\dot{\theta}^2\right) \tag{8}$$

$$E_{KV} = \frac{1}{2}M\dot{X}^2 + \frac{1}{2}I\dot{\theta}^2 \tag{9}$$

E_K is the kinetic-energy for the system

$$E_K = E_{KK} + E_{KV} \tag{10}$$

$$E_K = \frac{1}{2}m\left(\dot{X}^2 + 2l\dot{X}\dot{\theta}\cos\theta + l^2\dot{\theta}^2\right) + \left(\frac{1}{2}M\dot{X}^2 + \frac{1}{2}I\dot{\theta}^2\right)$$

∴ After simplifying the system, the total kinetic energy is

$$E_K = \frac{1}{2}(M+m)\dot{X}^2 + \frac{1}{2}\left(I+ml^2\right)\dot{\theta}^2 + ml\dot{X}\dot{\theta}\cos\theta$$

Equation of Lagrange for the velocity of the cart (X) and the angle of the pendulum θ that describe the system motion of inverted pendulum are

$$\frac{d}{dt}\left(\frac{\partial E_K}{\partial\dot{X}}\right) - \frac{\partial E_K}{\partial X} = Q_X \tag{11}$$

$$\frac{d}{dt}\left(\frac{\partial E_K}{\partial\dot{\theta}}\right) - \frac{\partial E_K}{\partial\theta} = Q_\theta \tag{12}$$

The terms of above equations must calculate as follows

$$\frac{\partial E_K}{\partial\dot{X}} = (M+m)\dot{X} + ml\dot{\theta}\cos\theta \tag{13}$$

$$\begin{aligned}\frac{d}{dt}\left(\frac{\partial E_K}{\partial\dot{X}}\right) &= \frac{d}{dt}\left[(M+m)\dot{X} + ml\dot{\theta}\cos\theta\right] \\ &= (M+m)\frac{d}{dt}\dot{X} + ml\frac{d}{dt}\left(\cos\theta\dot{\theta}\right) \\ &= (M+m)\ddot{X} + ml\ddot{\theta}\cos(\theta) - ml\dot{\theta}^2\sin(\theta)\end{aligned} \tag{14}$$

$$\frac{\partial E_K}{\partial X} = 0 \tag{15}$$

$$Q_X = F - b_1\ddot{X} \tag{16}$$

Then the first Lagrange equations becomes

$$\begin{aligned}&\left[(M+m)\ddot{X} + ml\ddot{\theta}l\cos(\theta) - ml\dot{\theta}^2 l\sin(\theta)\right] - [0] \\ &= \left[F - b_1\dot{X}\right]\end{aligned} \tag{17}$$

$$(M+m)\ddot{X} + m\,l\,\ddot{\theta}l\cos(\theta) - m\,l\dot{\theta}^2 l\sin(\theta) - F + b_1\dot{X} = 0$$

$$\ddot{X} = \frac{-ml\ddot{\theta}l\cos(\theta)}{(M+m)} + \frac{ml\dot{\theta}^2 l\sin(\theta)}{(M+m)} + \frac{F}{(M+m)} + \frac{b_1\dot{X}}{(M+m)} \tag{18}$$

And 2nd equation calculated in same way

$$\frac{\partial E_K}{\partial\dot{\theta}} = \left(I+ml^2\right)\dot{\theta} + ml\dot{X}\cos\theta \tag{19}$$

$$\begin{aligned}\frac{d}{dt}\left(\frac{\partial E_K}{\partial\dot{\theta}}\right) &= \frac{d}{dt}\left[\left(I+ml^2\right)\dot{\theta} + ml\dot{X}\cos\theta\right] \\ &= \left(I+ml^2\right)\frac{d}{dt}\dot{\theta} + ml\frac{d}{dt}\left(\cos\theta\dot{X}\right) \\ &= \left(I+ml^2\right)\ddot{\theta} + ml\cos\theta\ddot{X} - ml\dot{X}\dot{\theta}\sin\theta\end{aligned} \tag{20}$$

$$\frac{\partial E_K}{\partial\theta} = -ml\dot{X}\dot{\theta}\sin\theta \tag{21}$$

$$Q_\theta = -mgl\sin\theta - b_2\dot{\theta} \tag{22}$$

Then the second Lagrange equations becomes

$$\begin{aligned}&\left[\left(I+ml^2\right)\ddot{\theta} + ml\cos\theta\ddot{X} - ml\dot{X}\dot{\theta}\sin\theta\right] - \left[-ml\dot{X}\dot{\theta}\sin\theta\right] \\ &= \left[-mgl\sin\theta - b_2\dot{\theta}\right]\end{aligned} \tag{23}$$

$$\left(I+ml^2\right)\ddot{\theta} + ml\cos\theta\ddot{X} + mgl\sin\theta + b_2\dot{\theta} = 0 \tag{24}$$

$$\ddot{\theta} = -\frac{ml\cos\theta\ddot{X}}{I+ml^2} - \frac{mgl\sin\theta}{I+ml^2} - \frac{b_2\dot{\theta}}{I+ml^2} \tag{25}$$

3. FRACTIONAL ORDER CALCULUS

Fractional Order (FO) differential and integral is a frequent branch of calculus in which the integer order of differential and integral is generalized to real. The FO calculus is an ideal technique to represent a real-time system with greater precision than the integer order [23]. The fractional order differentiator-integrator is represented by the continuous operator ${}_aD_\alpha^t$ as defined by [24, 25].

$$ {}_aD_\alpha^t = \begin{cases} \dfrac{d^a}{dt^a} & \alpha>0 \\ 1 & \alpha = 0 \\ \displaystyle\int_a^t (d\tau)^a & \alpha<0 \end{cases} \tag{26} $$

Where: a is Upper limit, t is Lower limit, and α is FO, $\alpha \varepsilon R^+$.

There are multiple mathematical definitions for FO calculus. The following three well-established are common and include 1) The definition of the Grunwald Letnikovi (G-L), 2) The definition Riemann Liouvillei (R-L), and 3) The Caputo (C) [26] as follows:

1. (G-L). $$ {}_aD_\alpha^t f(t) = \lim_{h\to 0} \frac{1}{h^\alpha} \sum_{r=0}^{\left[\frac{t-a}{h}\right]} (-1r)^r \binom{\alpha}{r} f(t-rh) \tag{27} $$

2. (R-L). $$ {}_aD_\alpha^t f(t) = \frac{1}{(\mathrm{rm}-\alpha)} \frac{d^m}{dt^m} \int_a^t (t-\tau r)^{m-\alpha-1} f(\tau) d\tau \tag{28} $$

3. (C). $$ {}_aD_\alpha^t f(t) = \frac{1}{(\mathrm{rm}-\alpha)} \int_a^t (rt-\tau)^{m-\alpha-1} f^m(\tau) d\tau \tag{29} $$

Where:

$f(t)$ is Applied function, α is FO, $\alpha \varepsilon R^+$, m is Integer part of α, $m\text{-}1 < \alpha < m$, $m \in N$, t is Lower limit, a is Upper limit.

$(\bullet)$: Euler's Gamma function such that: $(z) = \int_0^\infty e^{-t} t^{z-1} dt$, for each $z \in R$, $\binom{\alpha}{r}$ is the coefficient of binomial, $\binom{\alpha}{r} = \frac{(\alpha+1)}{j!(\alpha-\mathrm{r}+1)}$, [27].

In most applications, these definitions are the same (equivalent), but there are exceptions where there is a need to introduce some variability. For example, R-L is used in calculus, Caputo is employed in numerical integrations and physics, while G-L works perfectly in communications and control engineering field.

3.1. Fractional order controller

The FOPID controller is an expansion of the IOPID controller. The IOPID is a "three term controller" and the FOPID or ($PI^\lambda D^\mu$) is a "five term controller", because it includes an Integral of order (λ) and Derivative of order (μ) [28]. The block diagram of FOPID controller is shown in Fig. 2.

The differential equation which describes the FOPID controller in time domain is given by:

$$ U(t) = K_P e(t) + K_I D^\lambda e(t) + K_D D^\mu e(t) \tag{30} $$

The transfer function of FOPID in S-domain (Laplace) is. $G_C(s) = \frac{U(s)}{E(s)} = K_P + K_I s^{-\lambda} e(t) + K_D s^\mu e(t), (\lambda,\ \mu > 0)$

Where: $G_C(s)$ is the controller transfer function, $E(s)$ is error, $\lambda,\ \mu$ is the FO of s, $\lambda,\ \mu \in [0,\ 1]$, $U(s)$ is the controller output. An IOPID controller is appeared into four points (P, PI, PD, PID), whereas FOPID controller is extended to a plane, so the classical PID is a special case of FOPID ($PI^\lambda D^\mu$) controller, as shown in Table 2 and Fig. 5.

4. FUZZY LOGIC CONTROLLER

Fuzzy logic controllers are a class of fuzzy logic-based controlling systems. A fuzzy logic is a mathematical idea that the computer uses to deal with (truth degrees) rather than Boolean logic (true logic and false logic) or (1 and 0). In recent years, the use of fuzzy logic controller (FLC) having Control engineering was the most popular application.

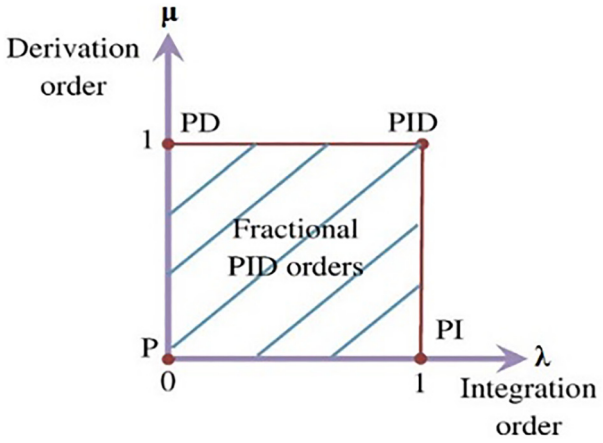

Fig. 3. Expansion of FOPID from four points to plan [24, 25]

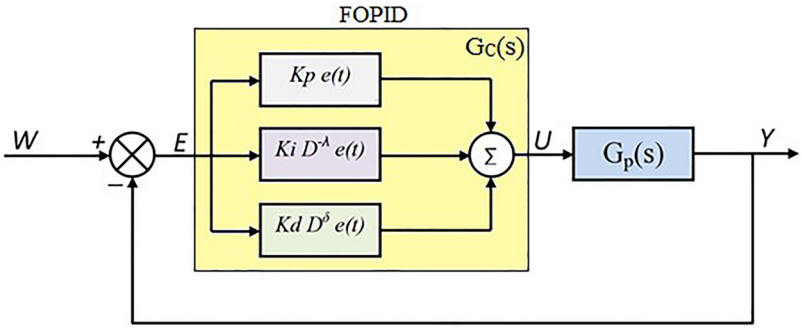

Fig. 2. Block diagram of FOPID controller [28]

The FLC is used instead of conventional controllers, like PID controller, to combine the benefits of classical controllers with the human intelligence. The first feature of a fuzzy logic controller is that it can be implemented to nonlinear models where the mathematical equations model is very hard to be derived. The second feature is that the fuzzy controller can be used to apply heuristic rules that contain the experiences of the human operators of system. The block diagram shown in Fig. 4 represent the structure of a FLS is.

The controller has two input and single output using Mamdani fuzzy set system type. The 2 I/P s' are the error and the change-of-error for pendulum angle $(e, \dot{e})$ and single output [29] represents the voltage of DC motor (V) as shown in Fig. 5.

5. EVOLUTIONARY ALGORITHMS FOR OPTIMIZATION

Choosing the appropriate (optimal value) settings for the any system controller is a difficult process. The outcomes can occasionally be poor, not because the controller is poorly constructed, but because the parameter values were not carefully chosen. Researchers on the subject of evolutionary algorithms studied the behavior of natural organisms and observed how they use intelligent mechanisms, especially their social behavior, such as flocks of birds or colonies of ants or bees. This research presents four types of evolutionary optimization algorithms. The first one is the Genetic Algorithm GA, the second is the Particle Swarm Optimization PCO, the third is the Ant Colony Optimization ACO and the fourth is the Social Spider Optimization SSO.

5.1. Genetic algorithm

The Genetic Algorithm (GA) takes its main lines from biological development laws [29]. The GA is a powerful evolutionary optimization approach that can optimize even the most complicated systems to carry out a genetic algorithm, the choice parameters' codes set the principal solution outlined, either in binary form (0 and 1) or as a double string or 'chromosome'. Non-evolutionary methods differ from GA [30]. GA is a probabilistic algorithm rather than a deterministic one (depends on chance or randomization). Furthermore, instead of acting on the solutions themselves, it operates on an abstraction of the solution set. In addition, rather than looking for a single answer, it explores a population of solutions. Finally, GA works with fitness functions that do not have derivatives. The following is the implementation of GA as shown in Fig. 6 [31].

1. Look for the first pop (population).
2. Locate the pop's fitness feature.
3. Reproduce the pop. using the fittest parents from the last generation.
4. Using a random method, locate the place of crossing.
5. Determine whether a mutation happened and, if so, what the outcome was.
6. Repeat steps 2–6 with a fresh population until the logic requirement is satisfied.

5.2. Ant colony optimization

Ants' food-finding behavior inspired the ant colony optimization (ACO) algorithm [32]. Scientists analyzed the ant colony's complicated behavior and discovered that these behavioral patterns may be used to solve complex optimization issues. Designing evolutionary algorithms for optimization issues is shown by the ACO algorithm. Complex optimization issues have been solved using methods derived from the food-finding behavior of ant colonies.

5.2.1.. Ant colony procedure. Ants release a chemical termed a pheromone on their travels between the colony and the food source [32]. Ants interact with each other by leaving pheromones on their paths. This pheromone is detectable by other ants, and it influences their path

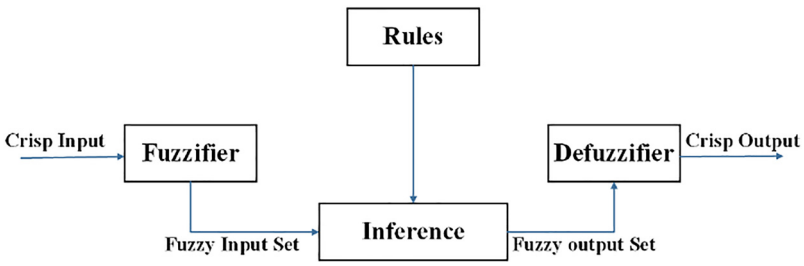

Fig. 4. General FLC block diagram

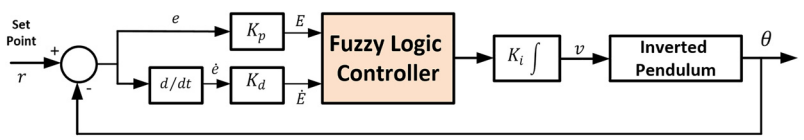

Fig. 5. The controller with fuzzy logic system

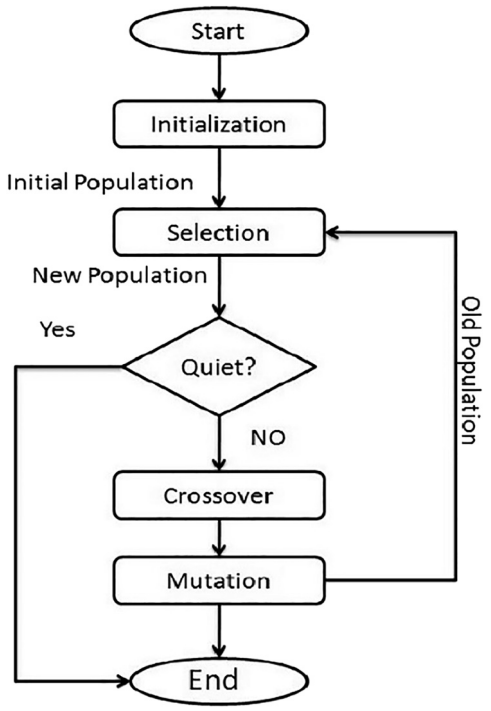

Fig. 6. GA flow chart [31]

choices. This indicates that the ants prefer to follow strong pheromone concentrations. The pheromones on the routes form "pheromone roadways," which show where good food supplies have already been discovered by other ants.

At all places along the route, the ACO utilizes adaptive pheromone adjustment, as may be seen in Fig. 7. These spots were chosen using a probabilistic approach. The ants are directed by a probability to choose the optimal course, which is referred to as a tour.

5.3. Particles swarm optimization

Particle Swarm Optimization (PSO) is an evolutionary stochastic optimization algorithm based on a population guided by the behavior of intelligent swarm behavior of some animals, such as bird flocks or fish schools [33–35]. Particle swarm optimization algorithm can be briefly explained as follows: It is a search operation by use of a swarm, such as that every single element in the swarm is called (a particle) and each particle may include the probable solution of the optimized case in the search space. PSO can keep the best global position of the swarm and that of its particle himself, and memorize the velocity also. In each iteration, the particle data is evaluated to adjust the velocity. Then that is used to calculate the new local position of the particle. Particle positions and velocities are changing constantly in the demanded search space until they reach the optimal state. A unique communication among the variant dimensions of the search space is provided by the objective functions. Experimental research showed that the PSO algorithm is a successful optimization tool [36–38].

The particles position is calculated as follows:

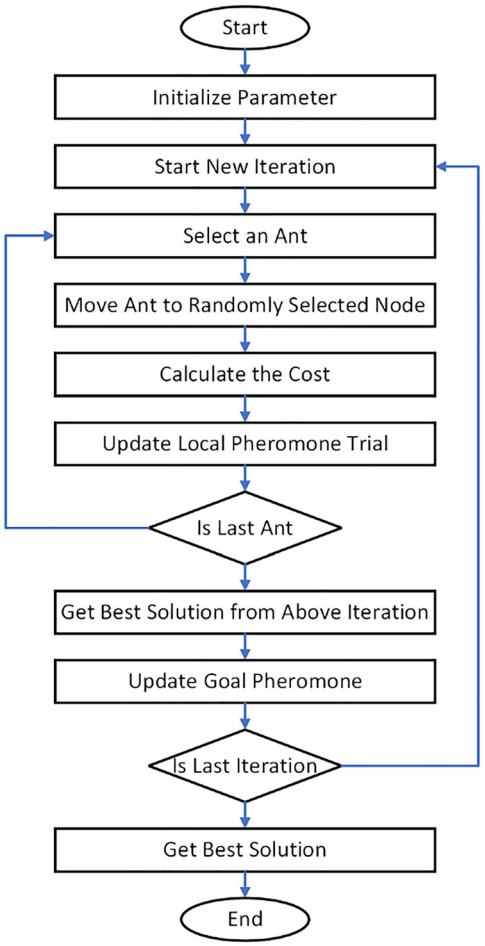

Fig. 7. ACO flow chart [32]

$$x_{ij}^{t+1} = x_{ij}^{t} + v_{ij}^{t+1} \tag{31}$$

The particles velocity is updated as follows:

$$v_{ij}^{t+1} = \mathrm{w}v_{ij}^{t} + c_1 r_{1j}^{t}\left[p_{best,i}^{t} - x_{ij}^{t}\right] + c_2 r_{2j}^{t}\left[G_{best} - x_{ij}^{t}\right] \tag{32}$$

Such that:

v_{ij}^{t} : Particle position, x_{ij}^{t}: Particle velocity, $p_{best,i}^{t}$ is Personal best position of particle, G_{best} : Global best position of particle, c_1, c_2 : Cognitive and social parameters, r_{1j}^{t}, r_{2j}^{t} : Random numbers between (0 and 1).

Fig. 8 shows a flowchart of the PSO algorithm.

5.4. Social Spider Optimization (SSO)

The SSO is a cooperative features in the spider colony society-inspired evolutionary optimization approach. The space of components in the SSO is a spiders collection that act in concert to mimic the natural socializing for a colony of spider. Each member of the colony is produced by comparable behaviors and traits in the majority of evolutionary swarm algorithms, whereas SSO employs two different elements: female and male. As a result, the job is determined by gender. Every piece functions as a separate activity in the colony of spiders, simulating its natural behavior. Most

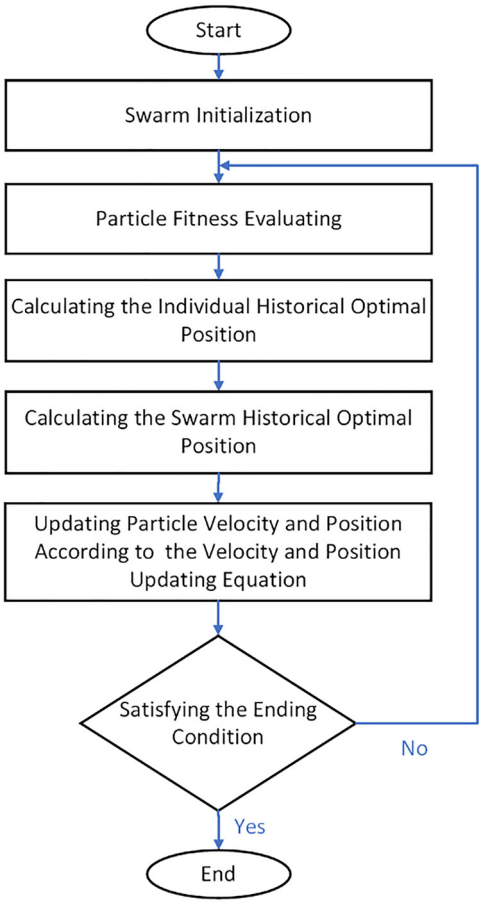

Fig. 8. Particle swarm optimization (PSO) Flow Chart

evolutionary algorithms have serious flaws, and this element separation improves them. As a result, the SSO has been refined and applied in a variety of technical domains. The method assumes that the components all behave like common spiders, and that each possible solution is a single spider [39, 40]. SSO was created to solve non-linear problems with constraints, as seen in the equation below:

$$\min.(f(x)); \quad xx = (xx^{i}, x^{2}, x^{3}, \ldots, x^{d}) \in R^{d}; \quad x \in X.$$

Where $f : R^{d} r \rightarrow R$ function is nonlinear,

$X = \{x \in rR^{d} \mid I_h \leq x \leq u_h, h = 1, \ldots, dd\}$ represent a minimized productized search space that is limited with a low (I_h) and by up (u_h) boundaries.

The SSO method finds optimum solutions for the search issue by searching a search space (S) from (N) possible solutions. To replicate a true colony, each answer appears as a separate element, space X perceives the entire society as a problem, with the female spiders number (N f) randomly selected from a total space S (65–95%), while the remaining (Nm) representing the number of male spiders,

$$(N_m = S - N_f).$$

Thus, the set (F_s) represents female elements $(F_s = \{fs_1, fs_2, \ldots, fs_{Nf}\})$, thus, the Ms group, represent the male elements, $(Ms = \{ms_1, ms_2, \ldots, ms_{nm}\})$, Such that

$$S = Fs \cup Mss$$

$$S = \{ss_1, s_2, \ldots, s_{Nn}\}$$

In SSO, each one element takes a value of weight (we_i) for it is fitness function, this weight is calculated by:

$$\mathrm{we}_i = \frac{\mathrm{fit}_i - \mathrm{Worst}}{\mathrm{Best} - \mathrm{Worst}}$$

such that (fit_i) .is a fitness function for $(i-i\mathrm{th})$. element position, $\{i \in (1, \ldots, N)i\}$Best is the best case of the fitness value of the entire space. Worst is the worst case of fitness for the entire population.

The social spider algorithm's core strategy is to exchange transition information. This exchange is carried out via vibrations on the spider web. The vibration from a spider I that is perceived by a spider (j) will be emulated and modelled by:

$$V_{i,j} = We_j \, e^{d_{i,j}^2}$$

such that (We_j) is a (j_{th}) the weight of the spider, (d) is the distance. from the 1st spider (i) to the 2nd spider (j).

Each first element (i) understands (3) methods only for web vibration, $(V_{i,j}, V_{i,b}$, and $V_{i,ff})$, such that $(V_{i,n})$ represents a vibration that is performed by the closest to element n by an upper weighting according to $(W_n - W_i)$. $(V_{i,f})$ is carried out by the closest to female elementi. It's applicable if (i) spider represents the male elementi. And $(V_{i,b})$ carried out by the best element in the space (S).

From a 1st stage $(k = 0)$ through a set number of loops $(k = it)$, SSO implements a population of elements space. All spiders are governed by a different group of evolutionary mechanisms depending on their gender. With female elements, the new location (fs_i^{K+1}) is achieved by updating the position of the current element (fs_i^K). The movement is accomplished with other spiders, and the updating procedure is controlled randomly by employing a probability factor (Pf). Furthermore, its vibrations are transmitted with the search space.

$$s_i^{K+1} = \begin{cases} fs_i^K + a.\mathrm{V}_{\mathrm{i,n}}.(s_n - fs_i^K) + \beta.\mathrm{V}_{\mathrm{i,b}}.(s_n - fs_i^K) + c.\left(\mathrm{rand} - \frac{1}{2}\right) \text{with probability}(\mathrm{P_f}) \\ fs_i^K + a.\mathrm{V}_{\mathrm{i,n}}.(s_n - fs_i^K) - \beta.\mathrm{V}_{\mathrm{i,b}}.(s_n - fs_i^K) + c.\left(\mathrm{rand} - \frac{1}{2}\right) \text{with}(1-\mathrm{P_f})\text{probability} \end{cases} \quad (33)$$

Such that (a, β, c) and (rand) are values chosen at random way $\in [0, 1]$,i (k) is the number of iterationi, (s_n) and (s_b) are individual elements symbolizing the closest element with a weight higher than (fs_i^K) and they are the best elements in the commune social spider respectively.

Also, the male element is categorized into two kinds: [dominant (D) and nondominant (ND)]. The male element whose fitness value is considered the best is the dominant for the overall male set and will integrate with the set. Following that, the (ND) set is constructed by the remainder of the male elements. With SSO technique, the (male) elements (ms_i^K) are offered with the following optimum equation:

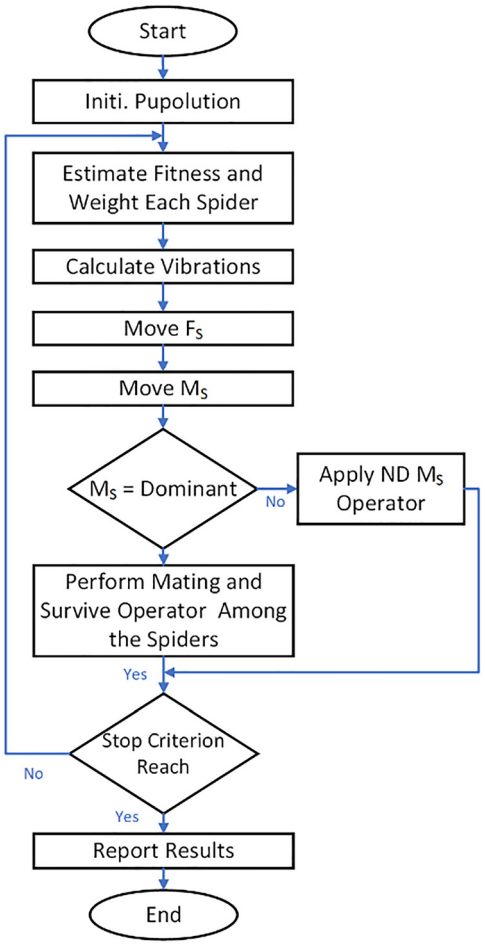

Fig. 9. SSO flow chart

$$fs_i^{K+1} = \begin{cases} ms_i^K + a \cdot V_{i,f} \cdot \left(s_f - ms_i^K\right) + c \cdot \left(rand - \frac{1}{2}\right) & if\ ms_i^K \varepsilon D \\ ms_i^K + a \cdot \left(\frac{\sum_{h \in ND} ms_i^K \cdot W_h}{\sum_{h \in ND} W_h} - ms_i^K\right) & if\ ms_i^K \varepsilon ND \end{cases} \quad (34)$$

(a, c) and (rand) :-randomly selected numbers $\in [0, 1]$. s_f is the nearest female element to the male spider (i).

The (mating operation) is employed between the dominant male spider (m_d) and the female element in the specified domain (r) in the social spider algorithm to generate a new spider (s_{new}). The probability of an impact on each element in (s_{new}) is determined by the weight of each element. The spider with the most weight has a higher chance of affecting the new spider (s_{new}). When a new element is created, it is compared to the rest of the population; if the new element is superior to the worst element in the population, the worst element is replaced with (s_{new}). Otherwise, it will be overlooked. Using a flow chart, Fig. 9 depicts the entire evolutionary process.

6. FOFPID CONTROLLER DESIGN

MATLAB (R2014a) Simulink used to design controller by a computer with CPU (Intel core i5), 2.53 GHz, 8 GB of RAM under Windowsi7 64_bit operating system. The design of FOFPID controller with the four algorithms (evolutionary optimization) SSO, PSO, GA, ACO as shown in Fig. 10.

As illustrated in Fig. 1, the number of membership functions (MF) for both the inputs and outputs is the same (7 MF) (Fig. 11).

The linguistic descriptions of membership functions are abbreviated as shown in Table 3 to keep it short but precise.

7. RESULTS AND DISCUSSIONS

7.1. Experimental InvPnd

Laboratory experiments were carried out on a digital pendulum system (Feedback Digital Pendulum 33-936) from Feedback Instruments Co., as shown in Fig. 12 [41, 42].

The cart runs in two opposite directions on a railway (1 m) and has two symmetrical pendulums attached to one axis allowing them to rotate together and free swing at 360°. The cart is connected to a DC motor located at the end of the rail by a toothed belt. The pulling force (F) of the vehicle is controlled by the voltage control (V) placed on the motor,

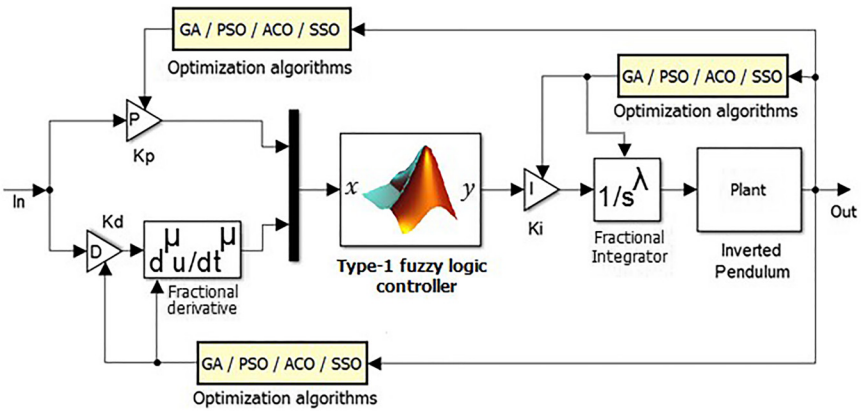

Fig. 10. FOT1FLC controller structure with four EO algorithm

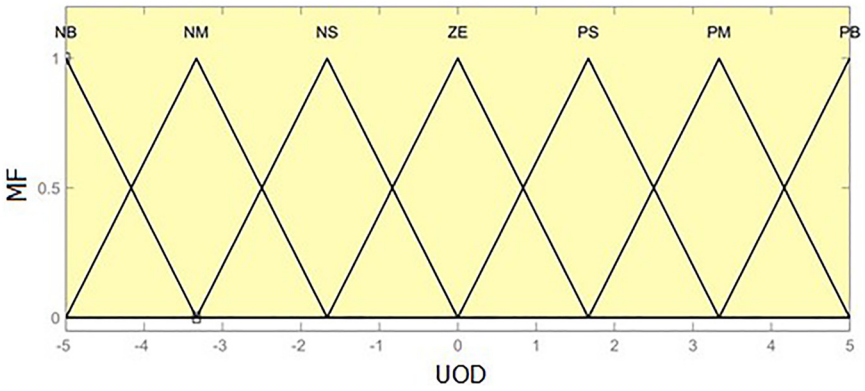

Fig. 11. T1FLC membership functions of error & change error input variable

Table 3. Abbreviation for linguistics description

Item	Linguistics description	Linguistics abbreviation
1	Negative-Big	N-B
2	Negative-Medium	N-M
3	Negative-Small	N-S
4	Zero-Error	Z-E
5	Positive-Small	P-S
6	Positive-Medium	P-M

Table 4. Fuzzy rule base

E.C/ E	N-B	N-M	N-S	Z-E	P-S	P-M	P-B
N-B	N-B	N-B	N-B	N-B	N-B	N-M	Z-E
N-M	N-B	N-B	N-B	N-B	N-M	Z-E	P-M
N-S	N-B	N-B	N-B	N-M	Z-E	P-M	P-B
Z-.E	N-B	N-B	N-M	Z-E	P-M	P-B	P-B
P-S	N-B	N-M	Z-E	P-M	P-B	P-B	P-B
P-M	N-M	Z-E	P-M	P-B	P-B	P-B	P-B
P-B	Z.-E	P-M	P-B	P-B	P-B	P-B	P-B

meaning that the force value is proportional to the value of the voltage. Sensors determine the location of vehicle (X) and the angle of the pendulum (θ) using an optical encoder [35,36]. Fig. 13 shows a control system scheme.

7.2. Type-1 fuzzy logic controller

T1FLC results using four evolutionary optimization algorithms, (GA, ACO, PSO, and SSO) and the comparison among them for parameters tuning are shown in Fig. 14.

The result show that clearly the T1FLC and SSO perform the best in regards of the peak value, peak time and oscillation.

7.3. Type-1 fuzzy logic controller with fractional order

The results of FOT1FLC employing four evolutionary techniques (GA, PSO, ACO, and SSO), as well as a comparison of the algorithms for parameter tuning, are displayed in Fig. 15. The results reveal that the FOT1FLC with SSO has the best peak time, peak value, and settling time features.

7.4. Comparison between T1FLC & FOT1FLC

Figure 16 below is comparing between T1FLC and FOT1FLC with the SS EO algorithm. The time response

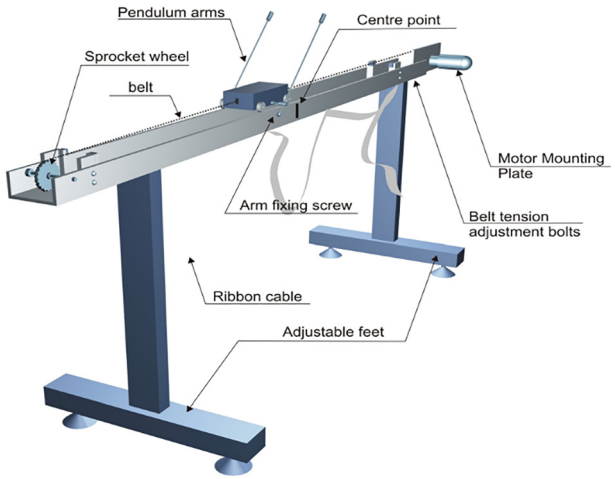

Fig. 12. Experimental system –Feedback Digital Pendulum [41, 42]

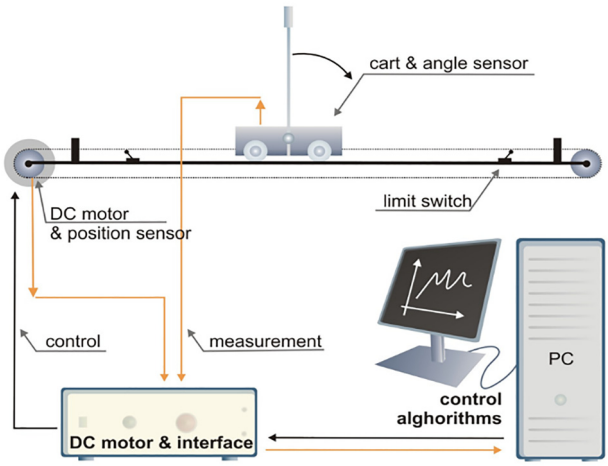

Fig. 13. Control system scheme [35]

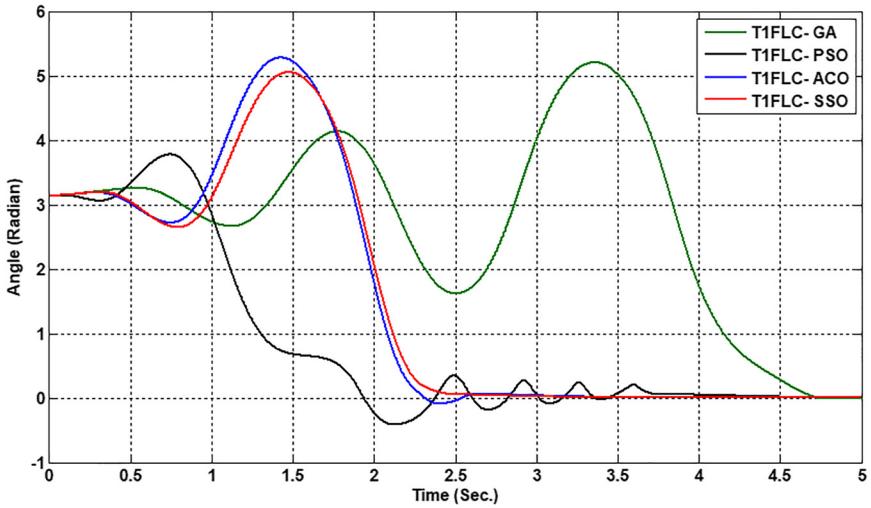

Fig. 14. Comparison between the four EO algorithms with T1FLC's

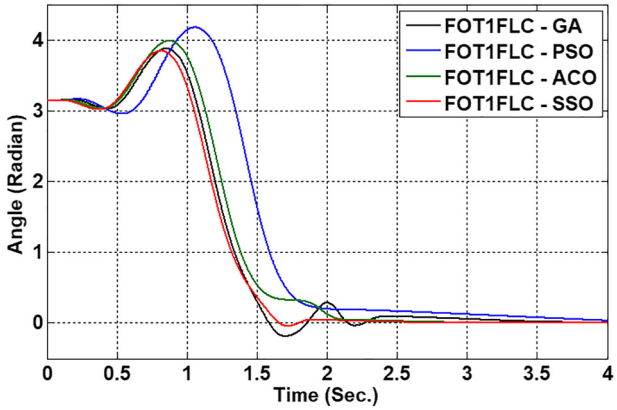

Fig. 15. Comparison among FOT1FLC's with the four EO's

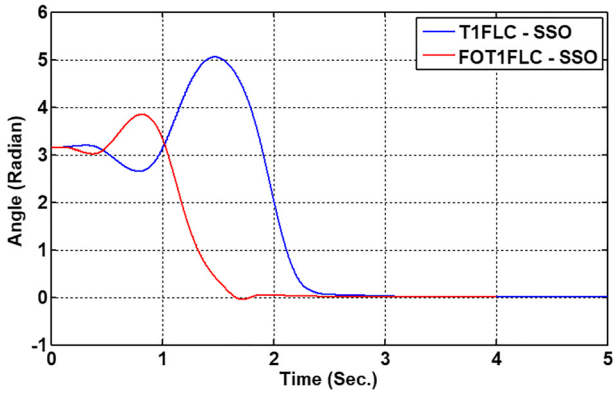

Fig. 16. Comparison between T1FLC and FOT1FLC with SSO

Table 6. The optimum paramters of T1FLC & FOT1FLC with SSO

Title	T1FLC	FOT1FLC
Kp	17.000	2.00647
Ki	2.8986	4.20972
Kd	0.5870	39.0594
λ	——	0.98977
μ	——	0.70524
Tuning time (min.)	70.287	109.384

graphs prove clearly that there is a strong influence for using the fractional-order instead of integer-order on the T1FLC structure. All the time response characteristics are reduced.

Table 5 combines the major characteristics of the two controllers using the four evolutionary algorithms with enhancement percentage between the two controllers.

Table 6 shows the optimum paramters of the two controllers T1FLC & FOT1FLC with SSO only. Fig. 17 is a chart represents the improvent in characteristics between T1FLC & FOT1FLC with SSO only.

8. CONCLUSIONS

The IOFLC and FOFLC controllers were utilized to run an inverted-pendulum-system on a cart using a (a digital pendulum control experimental system-33-936-S), and the controller's (Gains) parameter were optimized using four evolutionary optimizations (GA), (PSO), (ACO), and (ACO)

Table 5. Comparison among the two controllers T1FLC & FOT1FLC with the four evolutionary algorithms

Title	GA.			PSO.			ACO.			SSO.		
	T1FLC	FOT1FLC	Enh.%	T1FLC	FOT1FLC	Enh.%	T1FLC	FOT1FLC	Enh.%	T1FLC	FOT1FLC	Enh.%
Rise Time (sec.)	3.5508	0.3893	**89%**	1.5879	0.4068	**74%**	1.7483	0.6627	**62%**	1.6202	0.4446	**73%**
Settling Time (sec.)	4.5164	2.0652	**54%**	2.1896	1.8773	**14%**	2.5489	1.953	**23%**	2.2652	1.569	**31%**
Peak Time (sec.)	3.3605	0.8555	**75%**	1.4	1.059	**24%**	1.7755	0.8745	**51%**	1.4755	0.8195	**44%**
Peak value	5.2015	3.8757	**25%**	5.0011	4.1749	**17%**	5.5737	3.9849	**29%**	5.0556	3.8439	**24%**

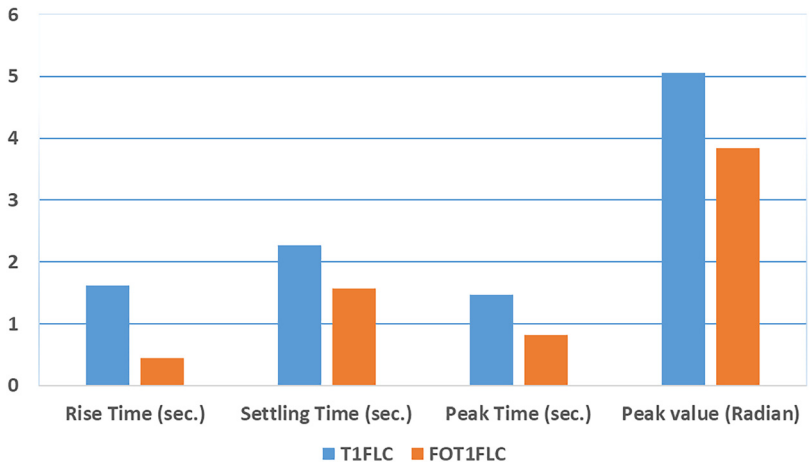

Fig. 17. The improvment in characteristics between T1FLC & FOT1FLC with SSO only

(SSO). The four evolutionary optimization techniques are compared to the results of tuned IOFLC and FOFLC with evolutionary optimization.

The comparisons between IOFLC and FOFLC, as well as different optimization strategies for each controller. The result appears that firstly the action of FOFLC is higher than the IOFLC along the four evolutionary optimization algorithms. Secondly FOFLC and SSO perform the best in settling time, peak time and peak value. The least tuning time is in (SSO) for both IOFLC and FOFLC. It's clearly the SSO is the best optimization algorithm. Other control techniques can be suggested for future work extension of this study and for the sake of comparison [43–45].

REFERENCES

[1] M. Magdy, A. El-Marhomy, and M. A. Attia, *Modeling of Inverted Pendulum System with Gravitational Search Algorithm Optimized Controller*. Cairo, Egypt: Dept. of Eng. Physics and Math., Faculty of Eng., Ain Shams University, January 2019.

[2] I. R. Ahmad, Y. Samer, and H. Al-Rizzo, *Fuzzy-logic Control of an Inverted Pendulum on a Cart*. Malaysia Campus, Malaysia: Dept. of Mechanical, Materials and Manufacturing Eng., The Univ. of Nottingham, July 2017.

[3] Y. Becerikli, and B. K. Celik, *Fuzzy Control of Inverted Pendulum and Concept of Stability Using Java Application*. Turkey: Kocaeli Univ., 15 December 2006.

[4] S. Irfan, A. Mehmood, M. T. Razzaq, and J. Iqbal, *Advanced Sliding Mode Control Techniques for Inverted Pendulum: Modelling and Simulation*. Pakistan: Dept. of Electrical Eng., COMSATS Univ., Islamabad, June 2018.

[5] P. Strakoš, and Tůma, *Mathematical Modelling and Controller Design of Inverted Pendulum*. Dept. of Control Systems and Instrumentation, VŠB-TU Ostrava, Czech Republic, IEEE, 2017.

[6] A. F. Ghalib, and A. F. Oglah, "Design and implementation of a fuzzy logic controller for inverted pendulum system based on evolutionary optimization algorithms," *Eng. Technol. J.*, vol. 38, No 3, pp. 361–74, 2020, Part A.

[7] J. Wang, *Simulation Studies of Inverted Pendulum Based on PID Controllers*. China: Hangzhou. Dianzi. Univ., August 2010.

[8] K. M. Passino, and S. Yurkovich, *Fuzzy Control*. Dept. of Electrical Eng., Ohio State Univ., Addison Wesley Longman, 1997.

[9] H. Y. Abed, A. T. Humod, and A. J. Humaidi, "Type 1 versus type 2 fuzzy logic speed controllers for brushless DC motors," *Int. J. Electr. Com. Eng.*, vol. 10, no. 1, pp. 265–74, 2020.

[10] G. V. Ochoa, J. D. Forero, and L. O. Quiñones, *Fuzzy Control of an Inverted. Pendulum Systems in MATLAB-Simulink, Efficient Energy Management Research Group -kai*. Colombia: Univ. of Atlántico km 7 Antigua vía Puerto, 2018.

[11] C. Wang, G. Yin, C. Liu, and W. Fu, *Design and Simulation of Inverted Pendulum System Based on the Fractional PID Controller*. Changchun Univ. of Science and Technology Dept. Changchun, IEEE, 2016.

[12] S. M. Abuelenin, *Decomposed Interval Type-2 Fuzzy Systems with Application to Inverted Pendulum*. Egypt: Eng. Faculty, Port-Said Univ., 2014, IEEE.

[13] A. M. El-Nagar, *Intelligent Control for Nonlinear Inverted Pendulum Based on Interval Type-2 Fuzzy PD Controller*. Egypt: Dept. of Industrial Electronics and Control Eng., Faculty of Electronic Eng., Menofia Univ., November 2013, Menof 32852.

[14] M. E. Abdela, H. M. Emara, and A. Bahgat, "Interval type 2 fuzzy sliding mode control with application to inverted pendulum on a cart," Electrical power and machines dept. Cairo Univ., Giza, Egypt, IEEE 2013.

[15] A. Kharola, and P. Patil, *PID Control of Two-Stage Inverted Pendulum*. Dehradun, India: Selçuk Univ. Mechanical Eng. Dept., Konya-Turkey Dept. of Mechanical Eng., Graphic Era Univ. (GEU), 2016, December, IEEE.

[16] I. Podlubny, *Fractional-order Systems and PIλDμ Controllers*. IEEE, 1999.

[17] P. warak, *Mathematical Modelling of Inverted Pendulum with Disturbance Input*. K.K.W. COE. &Research, Nashik, India, IRAJ, Oct. 2013.

[18] P. Strakoš, and J. Tůma, *Mathematical Modelling and Controller Design of Inverted Pendulum*. Department of Control Systems and Instrumentation, Ostrava, Czech Republic, IEEE, 2017.

[19] M. Magdy, A. El Marhomy, and M. A. Attia, "Modeling of inverted pendulum system with gravitational search algorithm optimized controller," *Ain Shams Eng. J.*, 2018, Elsevier.

[20] A. J. Humaidi, M. R. Hameed, A. R. Ajel, A. A. Al-Qassar, and I. K. Ibraheem, "Block backstepping control design of two-wheeled inverted pendulum via zero dynamic analysis," in *2021 IEEE 12th Control and System Graduate Research Colloquium*. vol. 2021, ICSGRC, 2021, pp. 87–92.

[21] A. J. Humaidi, A. A. Mohammed, A. H. Hameed, I. K. Ibrahim, A. T. Azar, and A. Q. Al-Dujaili, "State estimation of rotary inverted pendulum: a comparative study of observers performance," in *2020 IEEE Congreso Bienal de Argentina (ARGENCON)*. IEEE, 2020, pp. 1–7.

[22] A. J. Humaidi, E. N. Tala'at, M. R. Hameed and A. H. Hameed, "Design of adaptive observer-based backstepping control of cart-pole pendulum system," in *2019 IEEE International Conference on Electrical, Computer and Communication Technologies (ICECCT)*, 2019, pp. 1–5.

[23] M. Al-Dhaifallah, N. Kanagaraj, and K. S. Nisar, "Fuzzy fractional-order PID controller for fractional model of pneumatic pressure system", Electrical eng.g dept., college of eng. at wadi addawasir, KSA, Hindawi, 2018.

[24] H. N. Chaleshtori, S. M. A. Mohammadi, and E. Bijami, *Optimal Design of Fractional Order Fuzzy PID Controller with Simultaneous Auto-Tuned Fuzzy Control Rules and Membership Functions*. Dept. of Electrical Eng. Shahid Bahonar Univ. of Kerman, Iran, CSIEC, 20l7.

[25] J. Cao, J. Liang, and B. Cao, *Optimization of Fractional Order PID Controllers Based on Genetic Algorithms*. Dept. of mechanical eng., Xi'an Jiaotong Univ., China, IEEE, 2005.

[26] M. J. Mohamed, and A. Khashan, *Comparison between PID and FOPID Controllers Based on Particle Swarm Optimization", Control and Systems Eng.* Dept., univ. of technology Baghdad, Iraq, ECCCM2, 2014.

[27] H. M. Kadhim, and A. A. Oglah, "Interval type-2 and type-1 Fuzzy Logic Controllers for congestion avoidance in internet routers," *IOP Conf. Ser. Mater. Sci. Eng.*, vol. 881, no. 1, 2020, Art no. 012135.

[28] T. Ghanim, A. R. Ajel, and A. J. Humaidi, "Optimal fuzzy logic control for temperature control based on social spider optimization," *IOP Conf. Ser. Mater. Sci. Eng.*, vol. 745, no. 1, 012099, 2020.

[29] I. Abuiziah, and N. Shakarneh, *A Review of Genetic Algorithm Optimization: Operations and Applications to Water Pipeline Systems*. Institute of Agronomy and Veterinary Hassan II, Rabat, Morocco, IJPNSE, 2013.

[30] D. E. Gold Berg, *Genetic Algorithms in Search, Optimization, and Machine Learing*. Univ. of Alabama, January, 1989.

[31] B. Wu, C. Liu, X. Song, and X. Wang, *Design and Implementation of the Inverted Pendulum Optimal Controller Based on Hybrid Genetic Algorithm*. Institute of Electrical Eng., Hebei Univ. of Science and Technology, China, AMCCE, 2015.

[32] S. Katiyar, I. Nasiruddin, and A. Q. Ansari, *Ant Colony Optimization: a Tutorial Review*. New Delhi, India: Dept. of Electrical Eng., Jamia Millia Islamia, Aug 2015.

[33] A. J. Humaidi, S. K. Kadhim, and A. S. Gataa, "Development of a novel optimal backstepping control algorithm of magnetic impeller-bearing system for artificial heart ventricle pump," *Cybernetics Syst.*, vol. 51, no. 4, pp. 521–41, 2020.

[34] A. J. Humaidi, and A. F. Hasan, "Particle swarm optimization–based adaptive super-twisting sliding mode control design for 2-degree-of-freedom helicopter," *Meas. Control. (United Kingdom)*, vol. 52, nos 9–10, pp. 1403–19, 2019.

[35] A. J. Humaidi, H. M. Badr, and A. R. Ajil, "Design of active disturbance rejection control for single-link flexible joint robot manipulator," 2018 22nd International Conference on System Theory, Control and Computing (ICSTCC), 2018, pp. 452–7, 8540652.

[36] A. J. Humaidi, and H. M. Badr, "Linear and nonlinear active disturbance rejection controllers for single-link flexible joint robot manipulator based on PSO tuner," *J. Eng. Sci. Technol. Rev.*, vol. 11, no. 3, pp. 133–8, 2018.

[37] B. S. G. Almeida, and V. C. Leite, *Particle Swarm Optimization: a Powerful Technique for Solving Engineering Problems*. Federal Univ., of Rio de Janeiro, Brazil , IntechOpen, 2019.

[38] A. J. Humaidi, A. A. Oglah, S.J. Abbas, and I.K. Ibraheem, "Optimal augmented linear and nonlinear PD control design for parallel robot based on PSO tuner," *Int. Rev. Model. simulation*, vol. 12, no. 5, pp. 281–91, 2019.

[39] A. Luque-Chang, E. Cuevas, F. Fausto, D. Zald-var, and M. Pérez, *Social Spider Optimization Algorithm: Modifications, Applications, and Perspectives*. Dept. de electronica, univ. de Guadalajara, CUCEI, Mexico, Hindawi, Dec. 2018.

[40] A. J. Humaidi, H. T. Najem, A. Q. Al-Dujaili, D. A. Pereira, A. T. Azar, I.k. Ibraheem, "Social spider optimization algorithm for tuning parameters in PD-like Interval Type-2 Fuzzy Logic Controller applied to a parallel robot," *Meas. Control.*, vol. 54, nos 3–4, pp. 303–23, 2021.

[41] CO. Feedback, *Digital Pendulum Installation & Commissioning 33-936IC*. East Sussex, UK: Feedback Instruments Ltd..

[42] T. R. Krishnan, *On Stabilization of Cart-Inverted Pendulum System: An Experimental Study*. India: Dept. of Electrical Eng., National Institute of Technology, July, 2012.

[43] A. J. Humaidi and A. H. Hameed, "PMLSM position control based on continuous projection adaptive sliding mode controller," *Syst. Sci. Control. Eng.*, vol. 6, no. 3, pp. 242–52, 2018.

[44] A. J. Humaidi, M. R. Hameed, and A. H. Hameed, "Design of block-backstepping controller to ball and arc system based on zero dynamic Theory," *J. Eng. Sci. Technol.*, vol. 13, no. 7, pp. 2084–105, 2018.

[45] A. J. Humaidi and A. H. Hameed, "Robustness enhancement of MRAC using modification techniques for speed control of three phase induction motor," *J. Electr. Syst.*, vol. 13, no. 4, pp. 723–41, 2017.